ISSN 1330-3651 (Print), ISSN 1848-6339 (Online) https://doi.org/10.17559/TV-20231210001195
Original scientific paper

FEM Simulation of Rolling-Pressing Process with Horizontal and Vertical Rolls

Evgeniy PANIN*, Irina VOLOKITINA, Andrey VOLOKITIN, Abdrakhman NAIZABEKOV, Gulzhainat AKHMETOVA, Sergey LEZHNEV, Andrey TOLKUSHKIN, Aibol ESBOLAT

Abstract: In this work, finite element simulation of the rolling-pressing process with horizontal and vertical rolls was carried out. To analyze the efficiency of metal processing, the main parameters of the stress-strain state were considered: equivalent strain, equivalent stress, average hydrostatic pressure, deformation force. Aluminum alloy Al6063 was chosen as the workpiece material. For variational simulation, models with a change in the heating temperature of the workpiece and the rolls rotation speed were constructed. The most optimal option is a model in which the workpiece was heated to 100 °C and deformation was carried out at a circumferential speed of the first pair of rolls of 60 rpm. Variants with a single temperature reduction to 20 °C, or rotation speed reduction to 35 rpm also give acceptable results to all the indicators considered. However, rotation speed reduction to 10 rpm makes it impossible to carry out a stable process at any temperature.

Keywords: combined process; ECAP; FEM; force; rolling; simulation; stress-strain state

1 INTRODUCTION

Scientific works on obtaining high-quality metal with various methods of severe plastic deformation (SPD) are among the most cited publications in the world [1-3]. The SPD implementation due to the intensification of shear and alternating strains makes it possible to achieve the refinement of the initial structure to an ultrafine-grained state and obtain unique mechanical characteristics, which are sometimes paradoxical [4-5]. At the same time, the most well-known SPD methods high-pressure torsion (HPT) and equal-channel angular pressing (ECAP), allow deforming samples of limited geometric dimensions, which significantly reduces the possibility of using these methods on an industrial scale [6-9].

To overcome this limitation, in recent years, studies of new SPD processes have been conducted in various directions. One of such directions is the development of new deformation schemes of massive workpieces processing during forging [10-12], the key feature of which is an increased level of metal processing due to shear and alternating strains.

Another direction of research is the development of new deformation schemes for long-length workpieces. One of the first such technologies are the Conform and Linex processes, modifications of which are being created at the present time [13, 14]. For the possibility of deformation of long-length samples, a number of ECAP-based combined processes have been developed, which also ensure the continuity of the process [15, 16].

Radial-shear rolling deserves a special mention as SPD method for deforming long workpieces [17-19]. This method makes it possible to obtain an ultrafine-grained structure in the cross section of the rod in several passes, however, due to the complex turbulent metal flow, such structure is formed mainly in the surface layers, i.e. a gradient structure is created. At the same time, it is often necessary not only to grind the original grain size, but also to make the structure uniform in cross-section. From this point of view, a promising method is the «rolling-ECAP» combined method of deformation, during which it is possible to obtain a UFG structure in non-ferrous metals and alloys [20, 21].

The purpose of this work was finite element simulation of the modified «rolling-ECAP» combined process, the key feature of which was the use of a combined configuration of horizontal and vertical rolls. Due to the fact that the rolls in this process ensure the continuity of the deformation process and the possibility of long blanks processing, the presence of a combined configuration of the rolls will allow the workpieces to be consistently deformed in height and width, reducing the deviation from the original shape of the section.

2 MATERIALS AND METHODS

In the course of earlier theoretical studies of the «rolling-ECAP» combined process [22], it was revealed that in order to carry out this process, it is necessary to overcome the resistance forces arising from the matrix. This can be achieved by increasing the force that occurs in the deformation zone during rolling in the rolls, the value of which, in turn, can be changed by varying factors such as the radius of the rolls and absolute compression during rolling. However, it is also necessary to take into account the influence of various technological factors, such as the workpiece temperature, the value of which influences on deformation resistance, friction coefficients in the rolls and the matrix, as well as some other geometric factors, such as the length of matrix channels.

Simulation of the «rolling-ECAP» process was carried out in the Deform software package. The geometric and technological parameters of the tool and the workpiece were pre-selected using an algorithm for calculating the process forces in order to obtain a workpiece with a cross section of 20 × 20 mm [21]:

- the diameter of the first pair of rolls is 400 mm;
- the diameter of the second pair of rolls is 440 mm;
- the width of the matrix channel is 22 mm;
- the height of the matrix channel is 20 mm;
- the length of the input and output channels of the matrix is 90 mm;
- the length of the intermediate channel of the matrix is 20 mm;
- absolute compression of the workpiece in the first pair of rolls of 5 mm.

- absolute compression of the workpiece in the second pair of rolls of 2 mm.

The initial blank had the original dimensions of 24 × 19 × 200 mm. A mesh of finite elements evenly distributed over the entire volume of the workpiece was applied to this model. The average size of the final element was 2,3 mm, the number of nodes was 13695, the number of elements was 54780.

Aluminum alloy Al6063 was chosen as the material workpiece at a temperature of 100 °C, which is recommended for heating this alloy before deformation in order to exclude the recrystallization effect [23]. The rheological properties of the material were taken from the Deform database. For modeling, it was decided to use a non-isothermal type of calculation, i.e. in addition to giving heat to the tool, the workpiece also gave heat to the environment, the temperature of which was 20 °C. The following values of the friction coefficients were taken: 0,5 in the rolls to ensure the maximum value of the rolling force; 0,1 in the matrix to ensure a minimum backpressure value.

Previously, laboratory studies of the «rolling-ECAP» process were carried out using a rolling mill with a roll rotation speed of 60 rpm. It was decided to use similar conditions, gradually lowering the circumferential speed of the rolls to assess the effect of the rotation speed on the parameters of the stress-strain state.

To speed up the calculation and improve accuracy, the principle of horizontal symmetry was used, i.e., ½ of the width of the workpiece was used (Fig. 1). In accordance with this principle, the modeling required the geometry of only one of the vertical rolls.

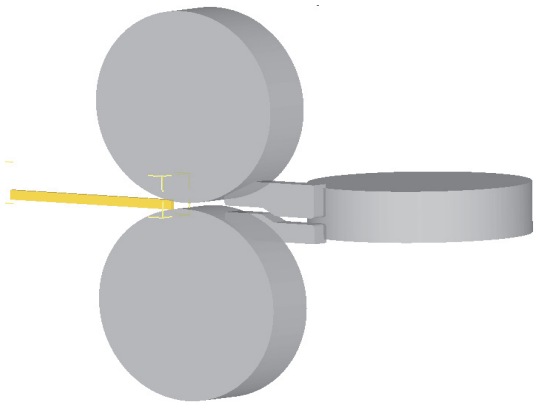

Figure 1 Initial model of the «rolling-ECAP» process with combined rolls

Taking into account the variation in the values of the heating temperature and the circumferential speed of the rolls, the following models were built:
1) with a workpiece heating temperature of 100 °C and a circumferential speed of the first pair of rolls of 60 rpm (basic model);
2) with a workpiece heating temperature of 100 °C and a circumferential speed of the first pair of rolls of 35 rpm;
3) with a workpiece heating temperature of 100 °C and a circumferential speed of the first pair of rolls of 10 rpm;
4) with a workpiece heating temperature of 20 °C and a circumferential speed of the first pair of rolls of 60 rpm;
5) with a workpiece heating temperature of 20 °C and a circumferential speed of the first pair of rolls of 35 rpm;
6) with a workpiece heating temperature of 20 °C and a circumferential speed of the first pair of rolls of 10 rpm.

In all models, the circumferential speed of the second pair of rolls was calculated according to the law of second volumes constancy after the front end of the workpiece fell into the output channel of the matrix, where the cross-sectional area of the workpiece was measured.

To analyze the strain state, it was decided to use an indicator of the intensity of strain, an equivalent strain Eq. (1), which gives an idea of the general level of study of the deformed material. To analyze the stress state, an indicator of stress intensity was used equivalent stress Eq. (2), showing the average level of all stresses, as well as the indicator "average hydrostatic pressure" Eq. (3), which in addition to stress values also takes into account their sign, which makes it possible to estimate the level of tensile and compressive stresses.

$$\varepsilon_{EQV} = \frac{\sqrt{2}}{3}\sqrt{(\varepsilon_1-\varepsilon_2)^2+(\varepsilon_2-\varepsilon_3)^2+(\varepsilon_3-\varepsilon_1)^2} \quad (1)$$

$$\sigma_{EQV} = \frac{1}{\sqrt{2}}\sqrt{(\sigma_1-\sigma_2)^2+(\sigma_2-\sigma_3)^2+(\sigma_3-\sigma_1)^2} \quad (2)$$

$$\sigma_{AV} = \frac{\sigma_1+\sigma_2+\sigma_3}{3} \quad (3)$$

where ε_1, ε_2, ε_3 - main strains, σ_1, σ_2, σ_3 - main stresses.

To assess the uniformity of the metal processing through the cross section, it was decided to consider these parameters at three points of the central section (Fig. 2). One point (point 2) was selected in the central area according to the workpiece height. Two other points (points 1 and 3) were selected in opposite surface areas. This choice is due to the fact that when passing through the matrix channels, the workpiece receives an inhomogeneous processing, therefore it is necessary to investigate the parameters of the stress-strain state over the entire workpiece height.

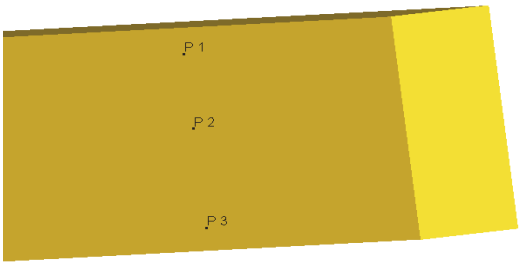

Figure 2 Location of control points in the workpiece section

3 RESULTS AND DISCUSSION

3.1 Basic Model "100 °C / 60 rpm"

Considering the distribution of equivalent strain, it is necessary to understand that this parameter has a cumulative character, i.e. it is accumulative and after removing the load its value does not decrease. A typical picture of the distribution of equivalent strain in the «rolling-ECAP» combined process is shown in Fig. 3. The zones of accumulation of strain are clearly visible on the workpiece as all the deformation zones pass sequentially.

For numerical estimation, we consider graphs of equivalent strain for the selected three points (Fig. 4). The selected zones I, II and III characterize the emerging zones of deformation of this combined process: I - the deformation zone in the first pair of rolls; II - the deformation zone in the inclined channel of the matrix; III - the deformation zone in the second pair of rolls. At the same time, it was revealed that the central zone of the workpiece receives a slightly higher level of processing than the surface layers. So, after leaving the second pair of rolls in the surface layers, the level of equivalent strain is 1,82 - 1,85, while in the central zone the level of equivalent strain reaches 2,3.

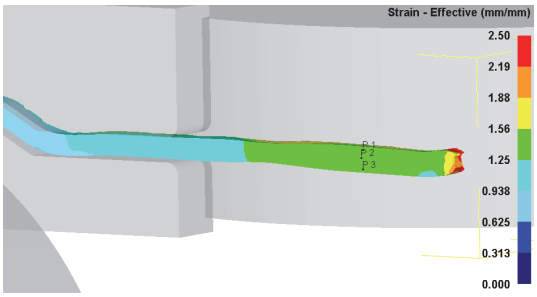

Figure 3 Equivalent strain distribution in "100 °C / 60 rpm"model

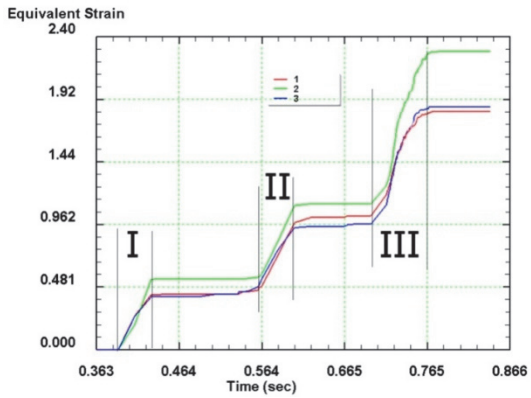

Figure 4 Graphs of equivalent strain in "100 °C / 60 rpm"model

Fig. 5 shows a typical picture of the equivalent stress distribution in the «rolling-ECAP» combined process. The parameters of the stress state are not accumulative, therefore, after leaving the deformation zone, the stress level decreases. To analyze the equivalent stress at the selected three points, consider the graphs on which the regions I, II and III were marked, characterizing the emerging geometric deformation zones (Fig. 6).

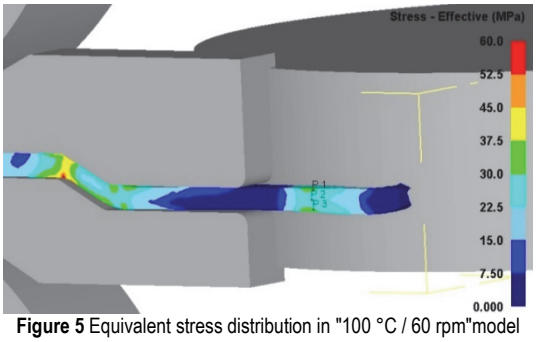

Figure 5 Equivalent stress distribution in "100 °C / 60 rpm"model

According to the curves in Fig. 6, it can be seen the extent of the physical deformation zones, since the stress actions in each of these three zones go beyond the geometric deformation zones. Here, the total stress level is 45 - 50 MPa in the deformation zone of the first pair of rolls; 35 - 45 MPa in the deformation zone of the matrix and 25 - 30 MPa in the deformation zone of the second pair of rolls. At the same time, the difference in stress values over the thickness of the workpiece is small and is 15% - 20%. It is also seen that the stress level in the deformation zone of the second pair of rolls is less than in the first pair of rolls. This is due to the fact that in order to ensure an optimal gripping angle and the necessary rolling force to pull the workpiece out of the die, a lower level of absolute compression is required, which is a consequence of the larger diameter of the rolls of the second pair.

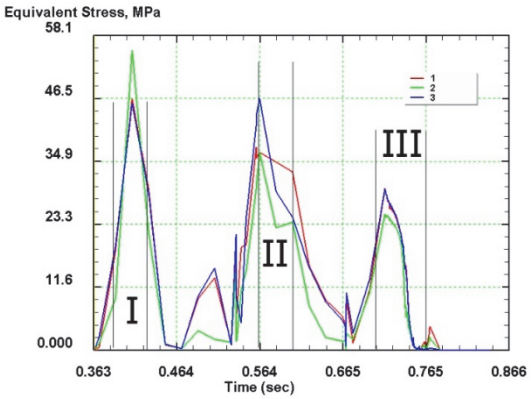

Figure 6 Graphs of equivalent stress in "100 °C / 60 rpm"model

Fig. 7 shows a typical picture of the distribution of the average hydrostatic pressure during the «rolling-ECAP» combined process. Here, the deformation zone in the rolls is covered by compressive stresses, whereas when moving along the channels of the matrix along the height of the workpiece, an alternating pattern occurs. At the first joint, when the workpiece is curved, compressive stresses occur on one side, and tensile stresses occur on the opposite side. At the second joint, the stress signs change, as the direction of curvature of the workpiece becomes reversed. To analyze the average hydrostatic pressure at the selected three points, consider the graphs in Fig. 8.

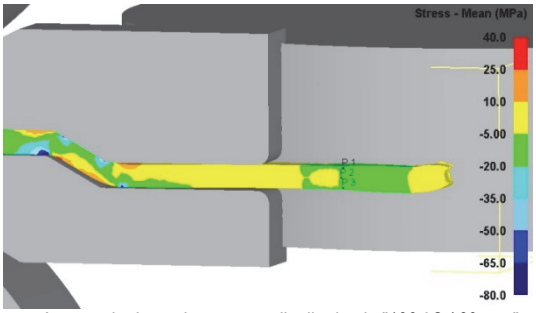

Figure 7 Average hydrostatic pressure distribution in "100 °C / 60 rpm"model

According to the curves in Fig. 8, it can be noted that in the deformation zones of both pairs of rolling rolls, the level of compressive stresses is approximately the same throughout the height of the workpiece, while in the first pair of rolls the level of compressive stresses is about 3 times higher than in the second pair of rolls (–30 MPa and –10 MPa). The deformation zone in the matrix can be divided into two stages. At the first stage, during the passage of the first channel junction, compressive stresses

of –75 MPa prevail on the lower face of the workpiece, while tensile stresses of 15 MPa occur on the upper face. At the second stage, during the passage of the second junction of the channels, due to the reverse direction of the flow, the stress signs change. Here, tensile stresses of 13 MPa occur on the lower face of the workpiece, while compressive stresses of –10 MPa occur on the upper face. At the exit from the second junction of the channels in the section of the workpiece, tensile stresses of 15 MPa act, however, the level of compressive stresses, compared with the entrance to this deformation zone, decreases to – 25 MPa, which is a consequence of some tension on the part of the second pair of rolls.

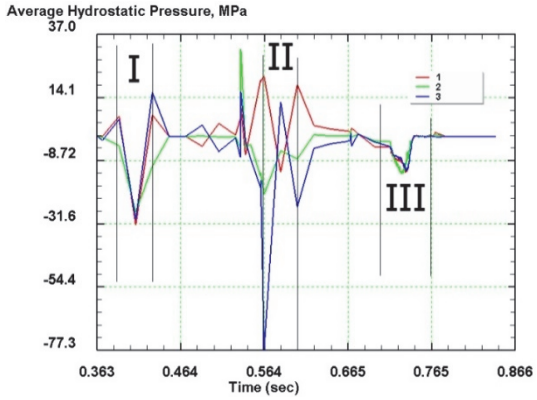

Figure 8 Graphs of average hydrostatic pressure in "100 °C / 60 rpm"model

Fig. 9 shows typical graphs of efforts during the «rolling-ECAP» combined process. The rolling force curves in the first pair of rolls have an almost uniform horizontal appearance. A small step of increasing the force characterizes the beginning of ECA-pressing in the matrix and the occurrence of backpressure from it.

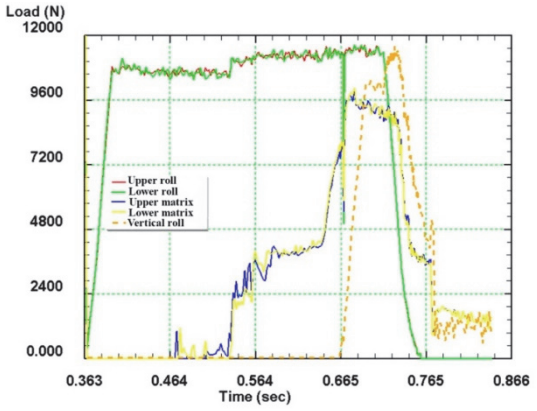

Figure 9 Force graphs in "100 °C / 60 rpm"model

The compression force curves in the matrix have a stepped appearance, which characterizes the passage of the workpiece along the channel joints. Also, from the joint consideration of the graphs of the rolling force and the ECAP, it can be noted that with a stable deformation process, the key condition of this process remains: the rolling force is greater than the pressing force. So, at the moment of the minimum force difference (when the workpiece is in all channels of the matrix), the rolling force is 11,5 kN, while the maximum pressing force is 9,5 kN. The dotted curve characterizes the rolling force in the second pair of vertical rolls. Here, the force is also greater than the pressing force and is 10 kN at the stage when the workpiece is in both pairs of rolls. After the workpiece exits the first pair of rolls, the force value increases slightly to 11,5 kN.

3.2 Model "100 °C / 35 rpm"

When the circumferential speed of the first pair of rolls decreases to 35 rpm, the overall strain rate decreases. This leads to a longer contact of the processed material with the matrix walls. In the case of a heated workpiece, this can lead to excessive cooling of the metal and a decrease in ductility. In our case, the heating temperature is not so significant that it is possible to talk about such an effect, however, the slow advance of the workpiece through the channels of the matrix can lead to an additional level of backpressure due to forced width compression.

Fig. 10 shows graphs of equivalent strain for the "100 °C / 35 rpm" model. Comparing these graphs with the values in the basic model, a slight increase in the length of the zones can be noted, which is a direct consequence of a decrease in the strain rate. At the same time, the central zone of the workpiece, as in the basic model, receives a higher level of processing than the surface layers. After leaving the second pair of rolls, the level of equivalent strain in the surface layers is 1,8 - 1,95, while in the central zone the level of equivalent strain reaches 2,2. A slight decrease in the level of strain in the central layer can be explained by a slower advance of the metal in all deformation zones, which affects the values of the metal flow velocity in the workpiece section. At the same time, an increase in the strain level on the upper face of the workpiece was indicated, which is the result of longer contact with the matrix walls than at the lower face.

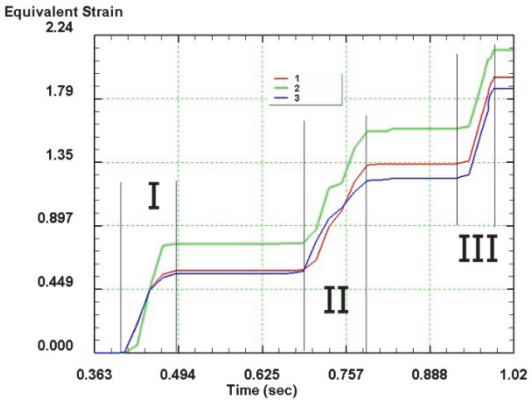

Figure 10 Graphs of equivalent strain in "100 °C / 35 rpm"model

Considering the equivalent stress curves in the "100 °C / 35 rpm" model in Fig. 11, a similar distribution of this parameter with the basic model can be noted. Three stress zones corresponding to deformation zones are also clearly visible here. At the same time, there is a slight increase in the overall stress level, which, as in the case of equivalent strain, is associated with an increase in the duration of deformation.

The total stress level is 60 - 65 MPa in the deformation zone of the first pair of rolls; 45 - 55 MPa in the deformation zone of the matrix and 30 - 35 MPa in the deformation zone of the second pair of rolls. As in the basic model, here the stress level in the deformation zone of the

second pair of rolls is less than in the first pair of rolls, which is associated with a lower level of absolute compression.

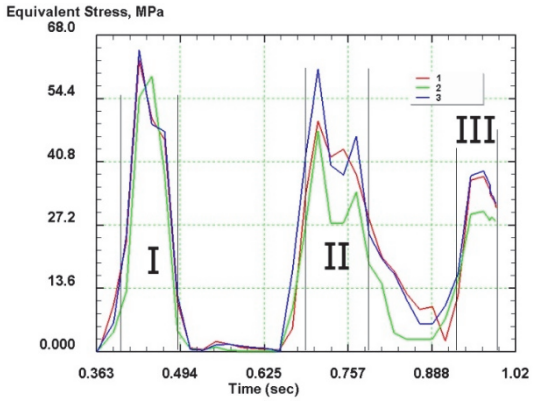

Figure 11 Graphs of equivalent stress in "100 °C / 35 rpm"model

Considering the curves of the average hydrostatic pressure in the model "100 °C / 35 rpm" in Fig. 12, the general similarity of the graphs with the basic model can be noted. However, due to a decrease in the strain rate in the deformation zones of both pairs of rolls, there is a significant increase in compressive stresses by 3 times (from –30 MPa to –90 - –95 MPa in the first pair of rolls and from –10 MPa to –25 - –28 MPa in the second pair of rolls).

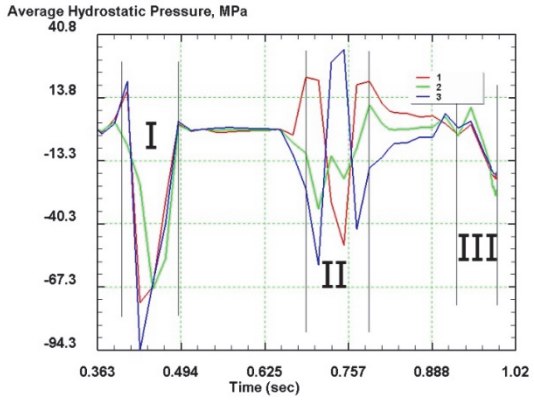

Figure 12 Graphs of average hydrostatic pressure in "100 °C / 35 rpm"model

The deformation zone in the matrix can also be divided into two stages. At the first stage, during the passage of the first channel junction, compressive stresses of –55 MPa prevail on the lower face of the workpiece, while tensile stresses of 25 MPa occur on the upper face. At the second stage, during the passage of the second channel junction, due to the reverse direction of flow, tensile stresses of 35 MPa arise on the lower face of the workpiece, compressive stresses of –45 MPa arise on the upper face. At the exit from the second junction of the channels, tensile stresses of 20 MPa act in the section of the workpiece, the level of compressive stresses is –40 MPa as in the basic model, there is also a tension effect from the second pair of rolls.

Fig. 13 shows the force graphs of the «rolling-ECAP» combined process for the "100 °C / 35 rpm" model. The nature of the rolling force curves in the first pair of rolls and pressing in the matrix have a form similar to the basic model. However, it should be noted here that due to a decrease in the rate of deformation and an increase in stresses, there is also an increase in the values of forces. At the same time, the stability condition of the process remains: the rolling force is greater than the pressing force, although the difference between them becomes minimal.

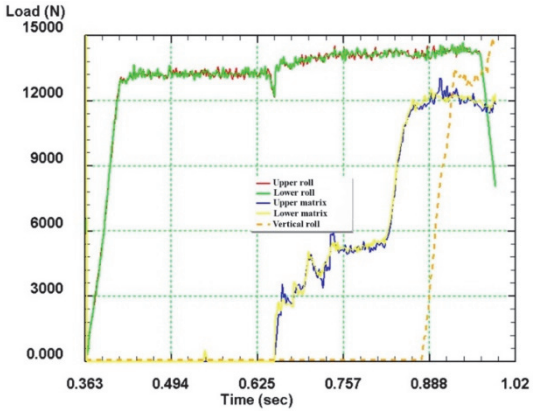

Figure 13 Force graphs in "100 °C / 35 rpm"model

When the workpiece is in all channels of the die, the rolling force is 14,8 kN, while the maximum pressing force is 12,8 kN. The rolling force in the second pair of vertical rolls is also greater than the pressing force and is 13,5 kN at the stage when the workpiece is in both pairs of rolls, as well as 15 kN after the workpiece exits the first pair of rolls.

3.3 Model "100 °C / 10 rpm"

A further decrease in the circumferential speed of the first pair of rolls to 10 rpm significantly increased the level of backpressure, which led to excessive compression of the workpiece and made the model unsuccessful (Fig. 14). When analyzing the similar «ECAP-Linex» process [14], with a decrease in the strain rate, such decompression did not occur due to the design feature of the process. Due to the fact that the chain pulleys were moving elements, the backpressure level of the «ECAP-Linex» process is significantly lower than in the «rolling-ECAP» process.

Also, an important reason for the decompression is the installation location of the matrix. Due to the increased level of backpressure in this combined process, rolls of a sufficiently large diameter are required, which limits the installation of the matrix near the vertical axis of the rolls. The presence of a free gap creates favourable conditions for the compression and curvature of the workpiece in it.

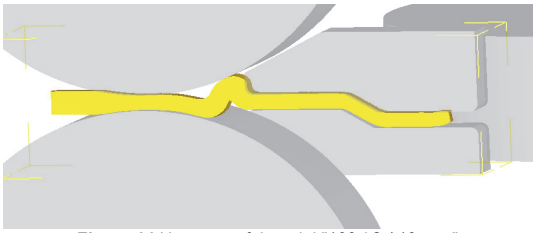

Figure 14 Unsuccessful model "100 °C / 10 rpm"

This effect is easily explained when considering the force graphs of the "100 °C / 10 rpm" model (Fig. 15). It can be seen here that with an increase in the overall level of effort, there was a violation of the stability condition of the process: the rolling force equalled the pressing force.

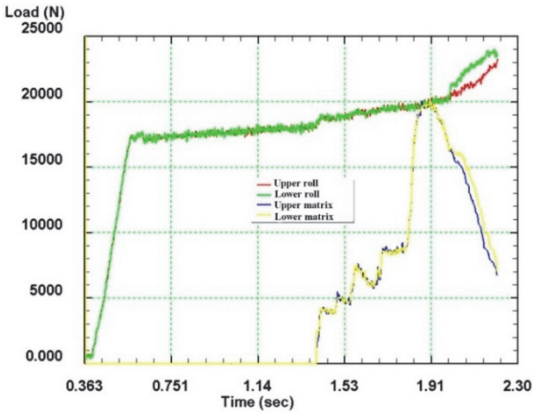

Figure 15 Force graphs in "100 °C / 10 rpm"model

As a corrective measure, it can be recommended changing the parameters that will lead to an increase in the rolling force: an increase in the diameter of the rolls or absolute compression. However, such variations in modeling are irrational, since they will require the modernization of equipment or the use of a new profile of the workpiece if necessary to obtain a given final section. Using a blank of the current dimensions with a new compression will result in a profile with other final dimensions, which is also not a rational solution.

3.4 Model "20 °C / 60 rpm"

In this model, the workpiece was not subjected to heating and deformed at ambient temperature. As a result, the processed alloy Al6063 had a reduced level of plasticity. As a result, after deformation there is a decrease in the overall level of equivalent strain (Fig. 16). Here, the amount of strain on the surface is 1,25 - 1,4, while in the center it reaches 1,6. At the same time, the general nature of the curves has a similar appearance to the previously considered models with a heated workpiece.

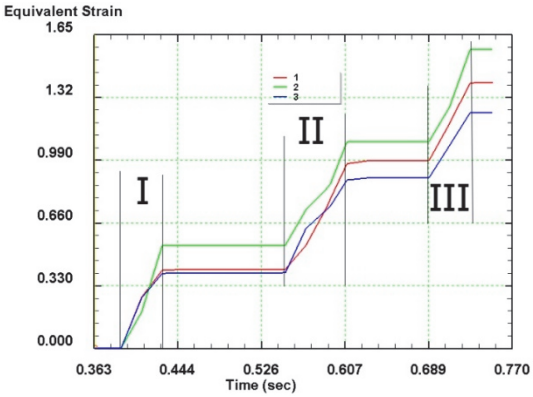

Figure 16 Graphs of equivalent strain in "20 °C / 60 rpm"model

Considering the equivalent stress curves in the model with a reduced workpiece temperature in Fig. 17, it can be noted a similar distribution of this parameter with models where the workpiece was heated. The graphs show three stress zones characterizing the deformation zones, but a decrease in the temperature of the workpiece leads to a general increase in stresses in all zones. The total stress level is 95 - 105 MPa in the deformation zone of the first pair of rolls; 65 - 75 MPa in the deformation zone of the matrix and 55 - 60 MPa in the deformation zone of the second pair of rolls.

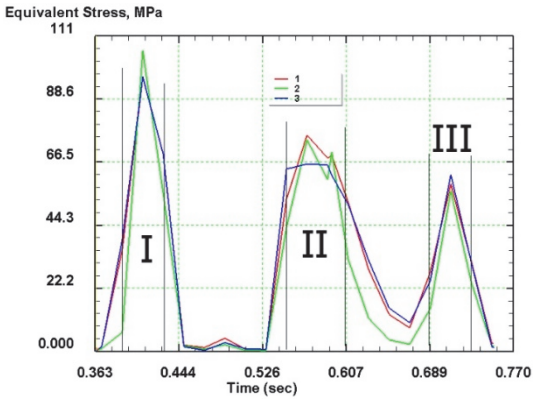

Figure 17 Graphs of equivalent stress in "20 °C / 60 rpm"model

Considering the curves of the average hydrostatic pressure in the model with a reduced workpiece temperature in Fig. 18, it can be noted the general similarity of the graphs with the previously considered models. Here, compressive stresses prevail in the deformation zones of the rolls, and in the matrix, with the sequential passage of two channel joints, the development of alternating stresses occurs. At the same time, a decrease in the temperature of the workpiece leads to an overall increase in both tensile and compressive stresses in all foci compared to the base model.

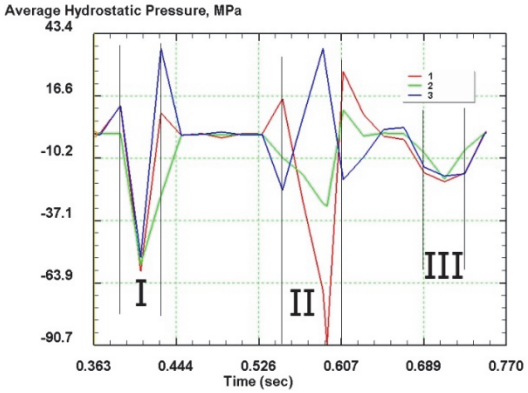

Figure 18 Graphs of average hydrostatic pressure in "20 °C / 60 rpm"model

In the deformation zones of the rolls, compressive stresses are observed at the level of –60 MPa in the first pair of rolls and –20 MPa in the second pair of rolls. In the matrix, during the passage of the first channel junction, compressive stresses of –25 MPa prevail on the lower face of the workpiece, while tensile stresses of 15 MPa occur on the upper face. During the passage of the second channel junction, due to the reverse direction of flow, tensile stresses of 40 MPa arise on the lower face of the workpiece, compressive stresses of –90 MPa arise on the upper face. At the exit from the second junction of the channels in the section of the workpiece, tensile stresses of 25 MPa act, the level of compressive stresses is –20 MPa.

Considering the force graphs in the model with a reduced workpiece temperature in Fig. 19, it can be noted that a decrease in the deformation temperature leads to an increase in stresses and, accordingly, to an increase in efforts.

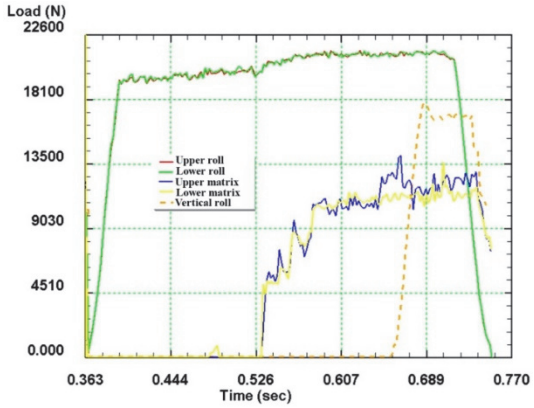

Figure 19 Force graphs in "20 °C / 60 rpm"model

The rolling force in the first pair of rolls reaches 21,7 kN, which is almost 2 times higher than the base value of 11,5 kN. The maximum pressing force is 13,6 kN, which is slightly different from the base value of 9,5 kN. The rolling force in the second pair of vertical rolls is 17,5 kN. At the same time, the stability condition of the process is maintained: the rolling forces are significantly greater than the pressing forces.

3.5 Model "20 °C / 35 rpm"

This model, in addition to the reduced value of the workpiece temperature, has a reduced circumferential speed of the rolls. These process conditions lead not only to a decrease in the plastic properties of the material, but also to an increase in backpressure due to an increase in the duration of contact with the matrix walls. In comparison with the "20 °C / 60 rpm" model, the overall level of equivalent strain in the central zone is slightly reduced from 1,6 to 1,5 (Fig. 20). The decrease on the surface faces is more significant – on the upper face, the value of equivalent strain decreased from 1,4 to 1,25; on the lower edge, this parameter decreased from 1,25 to 1,1.

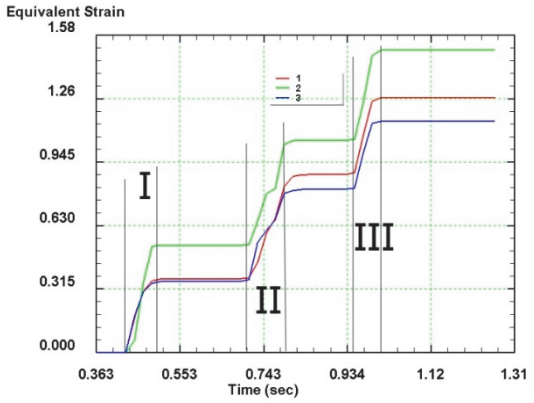

Figure 20 Graphs of equivalent strain in "20 °C / 35 rpm"model

Considering the curves of equivalent stress in the "20 °C / 35 rpm" model in Fig. 21, it can be noted that the simultaneous decrease in the temperature of the workpiece and the strain rate leads to a significant increase in stress compared to the base model. Under the given conditions, an increase in stresses is observed in all zones by more than 2 times, which amount to 110 - 120 MPa in the deformation zone of the first pair of rolls; 90 - 100 MPa in the deformation zone of the matrix and 65 - 75 MPa in the deformation zone of the second pair of rolls.

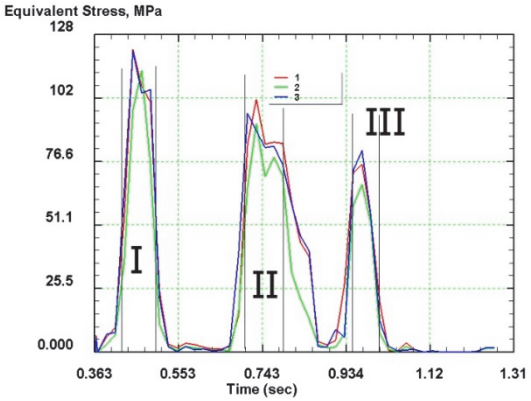

Figure 21 Graphs of equivalent stressin "20 °C / 35 rpm"model

Analyzing the curves of the average hydrostatic pressure in the "20 °C / 35 rpm" model (Fig. 22), it can be noted a similar increase in both tensile and compressive stresses in all deformation zones compared to the base model. At the same time, the nature of the stress distribution remains similar to the previously considered models.

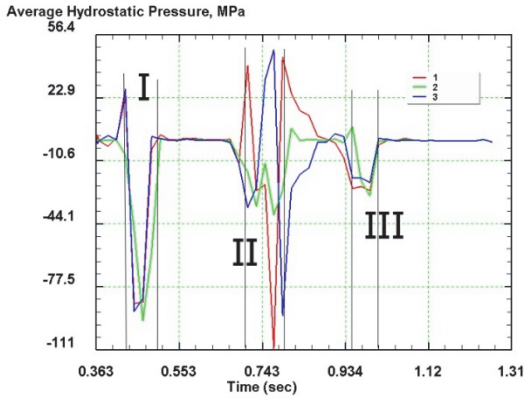

Figure 22 Graphs of average hydrostatic pressure in "20 °C / 35 rpm"model

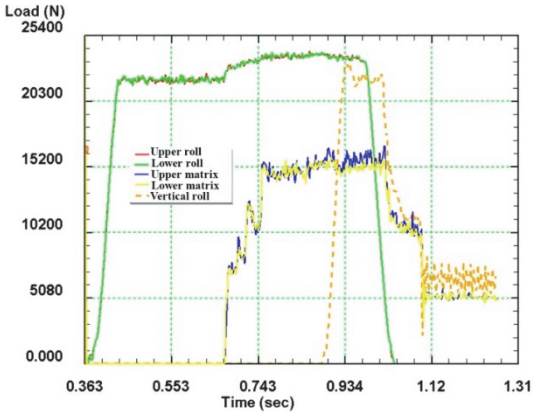

Figure 23 Force graphs in "20 °C / 35 rpm"model

In the deformation zones of the rolls, compressive stresses are observed at the level of –90 MPa in the first pair of rolls and –25 MPa in the second pair of rolls. In the matrix, during the passage of the first channel junction, compressive stresses of –40 MPa prevail on the lower face of the workpiece, while tensile stresses of 35 MPa occur on the upper face. During the passage of the second channel

junction, due to the reverse direction of flow, tensile stresses of 50 MPa arise on the lower face of the workpiece, compressive stresses of –110 MPa arise on the upper face. At the exit from the second junction of the channels in the section of the workpiece, tensile stresses of 45 MPa act, the level of compressive stresses is –90 MPa.

Considering the force graphs in the "20 °C / 35 rpm" model in Fig. 23, it can be noted that a simultaneous decrease in the temperature of the workpiece and the strain rate lead to an increase in effort. The rolling force in the first pair of rolls reaches 24 kN. The maximum pressing force is 16,3 kN. The rolling force in the second pair of vertical rolls at the time of simultaneous rolling of the workpiece by all rolls is 22,5 kN. The stability condition of the process is also preserved here: rolling forces are greater than pressing forces. However, the output of the workpiece from the first pair of rolls and the complete passage of the first joint of the channels, the rolling and pressing forces are almost equalized, which indicates the limiting stability conditions.

3.6 Model "20 °C / 10 rpm"

A further decrease in the circumferential speed of the first pair of rolls to 10 rpm and the lack of workpiece heating led to excessive backpressure from the matrix. As in the case of the "100 °C / 10 rpm" model, this caused the workpiece to be decompressed, which made the model unsuccessful (Fig. 24).

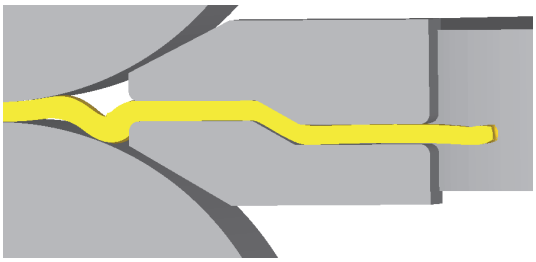

Figure 24 Unsuccessful model "20 °C / 10 rpm"

The study of the force graphs of the "20 °C / 10 rpm" model (Fig. 25) provides an answer to the cause of this phenomenon. It can be seen here that with an increase in the overall level of effort, there was a violation of the stability condition of the process: the pressing force exceeded the rolling force.

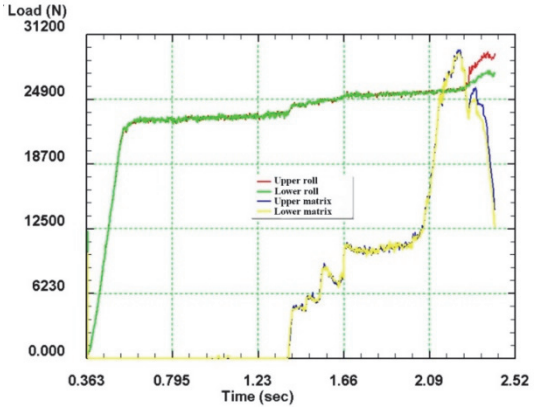

Figure 25 Force graphs in "20 °C / 10 rpm"model

3.7 Analysis of the Influence of Processing Factors on the Process Stability

To determine the analysis of the influence of the workpiece temperature and rolls rotation speed, it was decided to consider them in relation to the pressing force in the matrix to the rolling force in the rolls. To ensure stable deformation, this ratio must be less than 1. For this purpose, the value of this ratio has been determined for each model. In addition, the difference of each received value in relation to the base model was calculated. All results are presented in Tab. 1.

Table 1 Data for analysis

Model number	Temperature / °C	Rolls rotation speed / rpm	Ratio of the pressing force to the rolling force	Difference in relation to the basic model / %
1	100	60	9,5/11,5 = 0,826	100%
2	100	35	12,8/14,8 = 0,865	104,7%
3	100	10	20/20 = 1	121%
4	20	60	13,6/21,5 = 0,632	76,5%
5	20	35	16,3/24 = 0,679	82,5
6	20	10	29,9/26,1 = 1,14	138%

From the data obtained, it can be concluded that the greatest influence on the possibility of implementing the investigated combined process is a decrease in the rolls rotation speed to 10 rpm, which leads to the impossibility of stable deformation. At the same time, the other two speed values are characterized by the influence of the workpiece temperature, the use of the workpiece at ambient temperature significantly lowers the force ratio, which is expressed in an additional increase in reserve friction forces in the deformation zone of rolls. In addition, deformation of a colder workpiece has a lower risk of decompression at the entrance to the matrix, as evidenced by lower values of both force ratios and difference values relative to the basic model.

4 CONCLUSION

The purpose of this work was finite element simulation of the modified «rolling-ECAP» combined process, the key feature of which was the use of a combined configuration of horizontal and vertical rolls. To analyze the efficiency of metal processing, the main parameters of the stress-strain state were considered: equivalent strain, equivalent stress, average hydrostatic pressure and deformation force on the main elements of the combined process: two pairs of rolls and an equal-channel step matrix. For variational simulation, models with different heating temperature of the workpiece and rolls rotation speed were constructed.

The key parameter in metal forming processes is usually considered either the deformation force or the level of metal processing, which depends on the equivalent strain. From this point of view, the most optimal option is the model where workpiece was heated to 100 °C and deformation was carried out at a circumferential speed of the first pair of rolls of 60 rpm. Variants with a temperature reduction to 20 °C, or rotation speed reduction to 35 rpm also give acceptable results to all the indicators considered. However, rotation speed reduction to 10 rpm makes it impossible to carry out a stable process at any temperature.

The obtained simulation results will be the basis for the design of an experimental installation for the implementation of the rolling-pressing process.

Acknowledgements

This research was funded by the Science Committee of the Ministry of science and higher education of the Republic of Kazakhstan (Grant № AP13067723).

5 REFERENCES

[1] Valiev, R. Z., Islamgaliev, R. K., & Alexandrov, I. V. (2000). Bulk nanostructured materials from severe plastic deformation. *Progress in Materials Science, 45*(2), 103-189. https://doi.org/10.1016/S0079-6425(99)00007-9

[2] Valiev, R. Z. & Langdon, T. G. (2006). Principles of equal-channel angular pressing as a processing tool for grain refinement. *Progress in Materials Science, 51*(7), 881-981. https://doi.org/10.1016/j.pmatsci.2006.02.003

[3] Sakai, T., Belyakov, A., Kaibyshev, R., Miura, H., & Jonas, J. J. (2014). Dynamic and post-dynamic recrystallization under hot, cold and severe plastic deformation conditions. *Progress in Materials Science, 60*(1), 130-207. https://doi.org/10.1016/j.pmatsci.2013.09.002

[4] Tsuji, N., Ito, Y., Saito, Y., & Minamino, Y. (2002). Strength and ductility of ultrafine grained aluminum and iron produced by ARB and annealing. *Scripta Materialia, 47*(12), 893-899. https://doi.org/10.1016/S1359-6462(02)00282-8

[5] Valiev, R. Z., Alexandrov, I. V., Zhu, Y. T., & Lowe, T. C. (2002). Paradox of strength and ductility in metals processed by severe plastic deformation.*Journal of Materials Research, 17*(1), 5-8. https://doi.org/10.1557/JMR.2002.0002

[6] Zhilyaev, A. P. & Langdon, T. G. (2008). Using high-pressure torsion for metal processing: Fundamentals and applications. *Progress in Materials Science, 53*(6), 893-979. https://doi.org/10.1016/j.pmatsci.2008.03.002

[7] Emerla, M., Bazarnik, P., Huang, Y., Lewandowska, M., & Langdon, T. G. (2023). Using direct high-pressure torsion synthesis to produce aluminium matrix nanocomposites reinforced with carbon nanotubes. *Journal of Alloys and Compounds, 968*, 171928. https://doi.org/10.1016/j.jallcom.2023.171928

[8] Muñoz, J. A., Chand, M., Signorelli, J. W., Calvo, J., & Cabrera, J. M. (2022). Strengthening of duplex stainless steel processed by equal channel angular pressing (ECAP). *International Journal of Advanced Manufacturing Technology, 123*(7-8), 2261-2278. https://doi.org/10.1007/s00170-022-10311-2

[9] Zohrevand, M., Mohammadi-Zerankeshi, M., Nobakht-Farin, F., Alizadeh, R., & Mahmudi, R. (2022). Degradation behavior of the as-extruded and ECAP-processed Mg-4Zn alloy by Ca addition and hydrothermal coating. *Journal of Materials Research and Technology, 20*, 1204-1215. https://doi.org/10.1016/j.jmrt.2022.07.072

[10] Kukhar, V., Balalayeva, E., Hurkovska, S., Sahirov, Y., Markov, O., Prysiazhnyi, A., & Anishchenko, O. (2020). The selection of options for closed-die forging of complex parts using computer simulation by the criteria of material savings and minimum forging force. *Advances in Intelligent Systems and Computing, 989*, 325-331. https://doi.org/10.1007/978-981-13-8618-3_35

[11] Drahobetsky, V. V., Shapoval, A. A., Shchetynin, V. T., Argat, R. G., Shlyk, S. V., Mos'pan, D. V., Gorbatyuk, S. M., & Markov, O. E. (2022). New Solution for Plastic Deformation Process Intensification. *Metallurgist, 65*, 1108-1116. https://doi.org/10.1007/s11015-022-01253-x

[12] Markov, O. E., Khvashchynskyi, A. S., Musorin, A. V., Markova, M. A., Shapoval, A. A., & Hrudkina, N. S. (2022). Investigation of new method of large ingots forging based on upsetting of workpieces with ledges. *International Journal of Advanced Manufacturing Technology, 122*, 1383-1394. https://doi.org/10.1007/s00170-022-09989-1

[13] Ghaforian Nosrati, H., Gerdooei, M., Khalili, K., & Mohammadi, M. (2023). Usability of the ECAP-Conform process for the production of dental implants material. *Journal of the Mechanical Behavior of Biomedical Materials, 147*, 106124. https://doi.org/10.1016/j.jmbbm.2023.106124

[14] Panin, E., Volokitina, I., Volokitin, A., Naizabekov, A., Akhmetova, G., Lezhnev, S., Tolkushkin, A., Esbolat, A., & Yordanova, R. (2023). Finite Element Modeling of ECAP-Linex Combined Process of Severe Plastic Deformation. *Modelling and Simulation in Engineering, 2023*, 1573884. https://doi.org/10.1155/2023/1573884

[15 Chukin, M. V., Korchunov, A. G., Polyakova, M. A., & Emaleeva, D. G. (2010). Forming ultrafine-grain structure in steel wire by continuous deformation. *Steel in Translation, 40*(6), 595-597. https://doi.org/10.3103/S0967091210060203

[16] Konstantinov, D. V., Korchunov, A. G., Zaitseva, M. V., Shiryaev, O. P., & Emaleeva, D. G. (2018). Macro- and Micromechanics of Pearlitic-Steel Deformation in Multistage Wire Production. *Steel in Translation, 48*(7), 458-462. https://doi.org/10.3103/S0967091218070094

[17] Petrova, A. N., Rasposienko, D. Yu., Astafyev, V. V., & Yakovleva, A. O. (2023). Structure and strength of Al-Mn-Cu-Zr-Cr-Fe ALTEC alloy after radial-shear rolling. *Letters on Materials, 13*(2), 177-182. https://doi.org/10.22226/2410-3535-2023-2-177-182

[18] Lezhnev, S., Panin, E., Tolkushkin, A., Kuis, D., & Kasperovich, A. (2023). Development and computer simulation of a new technology for forming and strengthening screw fittings. *Journal of Chemical Technology and Metallurgy, 58*(5), 955-960. https://doi.org/10.59957/jctm.v58i5.132

[19] Mashekov, S., Nurtazaev, E., Mashekova, A., & Abishkenov, M. (2021). Extruding aluminum bars on a new structure radial shear mill. *Metalurgija, 60*(3-4), 427-430.

[20] Naizabekov, A., Lezhnev, S., Panin, E., Volokitina, I., Arbuz, A., Koinov, T., & Mazur, I. (2019). Effect of Combined Rolling–ECAP on Ultrafine-Grained Structure and Properties in 6063 Al Alloy. *Journal of Materials Engineering and Performance, 28*(1), 200-210. https://doi.org/10.1007/s11665-018-3790-z

[21] Naizabekov, A., Lezhnev, S., & Panin, E. (2019). Study of the Influence of the Main Parameters of "Rolling-ECAP" Process on the Stress-Strain State and the Microstructure Evolution Using Computer Simulation. *Procedia Manufacturing, 37*, 459-466. https://doi.org/10.1016/j.promfg.2019.12.074

[22] Panin, E., Lezhnev, S., Naizabekov, A., & Koinov, T. (2016). Theoretical grounds of the combined rolling - equal - channel step pressing process. *Journal of Chemical Technology and Metallurgy, 51*(5), 594-602.

[23] Sabirov, I., Perez-Prado, M. T., Murashkin, M., Molina-Aldareguia, J. M., Bobruk, E. V., Yunusova, N. F., & Valiev, R. Z. (2010). Application of equal channel angular pressing with parallel channels for grain refinement in aluminium alloys and its effect on deformation behavior. *International Journal of Material Forming, 3*(1), 411-414. https://doi.org/10.1007/s12289-010-0794-0

Contact information:

Evgeniy PANIN, PhD, associate professor
(Corresponding author)
Karaganda Industrial University,
101400, Kazakhstan, Temirtau, Republic avenue, 30
E-mail: ye.panin@tttu.edu.kz

Irina VOLOKITINA, PhD, associate professor
Karaganda Industrial University,
101400, Kazakhstan, Temirtau, Republic avenue, 30
E-mail: irinka.vav@mail.ru

Andrey VOLOKITIN, PhD
Karaganda Industrial University,
101400, Kazakhstan, Temirtau, Republic avenue, 30
E-mail: dyusha.vav@mail.ru

Abdrakhman NAIZABEKOV, Doctor of technical sciences, professor
Rudny Industrial Institute,
111500, Kazakhstan, Rudny, 50 let Oktyabrya, 38
E-mail: naizabekov57@mail.ru

Gulzhainat AKHMETOVA, PhD, associate professor
Karaganda Industrial University,
101400, Kazakhstan, Temirtau, Republic avenue, 30
E-mail: agulzhajnat@bk.ru

Sergey LEZHNEV, Candidate of technical sciences, professor
Rudny Industrial Institute,
111500, Kazakhstan, Rudny, 50 let Oktyabrya, 38
E-mail: sergey_legnev@mail.ru

Andrey TOLKUSHKIN, PhD student
Ural Federal University,
620002, Russia, Yekaterinburg, Mira street, 19
E-mail: a.o.tolkushkin@urfu.ru

Aibol ESBOLAT, PhD student
Karaganda Industrial University,
101400, Kazakhstan, Temirtau, Republic avenue, 30
E-mail: esbolat.a@mail.ru